

# Seismic anisotropy applied to geothermal prospection

R. Baillet, N. Desgoutte, V.Thomas and J. Caudroit

---

## Introduction

Anisotropy estimation allows to go beyond the lateral resolution of the conventional seismic data (Lui and Martinez, 2012); a full-stack full-azimuth seismic inversion and its associated characterization, as described in the previous chapter, assumes a homogeneous and isotropic medium. The proposed azimuthal approach allows us to overcome this limitation by estimating the key properties for each source/receiver direction. Small heterogeneities, such as smaller fractures, can be detected if the impedance varies from one sector to another, generating an azimuthal anomaly. The anisotropy magnitude and orientation can be extracted for further analysis and linked, if possible, to fracture intensity and orientation (Adelinet et al., 2012). This fracture intensity can have a major impact on the expected flow rate or communication between the reservoirs, and, therefore, is often a key element for decision making.

After elaborating briefly the technical background, we will describe the methodology for both VVAZ (Velocity versus Azimuth) and AVAZ (Amplitude versus Azimuth), based on partially stacked seismic according to the azimuth. The software used for the demonstration is InterWell, the software solution from

Beicip-Franlab, part of IFPEN group, able to extract anisotropy either for velocity or amplitude anomalies.

The use of the VVAZ – AVAZ methodology is illustrated by a practical case study in geothermal prospection in Geneva basin, Switzerland (Baillet and Caudroit, 2024).

## 8.1 Technical background

### 8.1.1 The HTI and VTI models for anisotropy models

A VTI media, standing for Vertical Transverse Isotropic, is characterized by horizontal layering, as evidenced in shale overburdens. The stiffening of the rock in the horizontal direction increases the P-wave velocity in this direction compared to vertical propagation. This model is suitable for lithology prediction.

On the other hand, a HTI media, standing for Horizontal Transverse Isotropic, is characterized by vertical layering, such as seen in a fractured reservoir. Here the rock is stiffer along the strike of the fractures giving the fastest P-wave velocity in this direction.

It is important to highlight that both AVAZ and VVAZ approaches are sensitive to both anisotropy models, represented Figure 8.1.

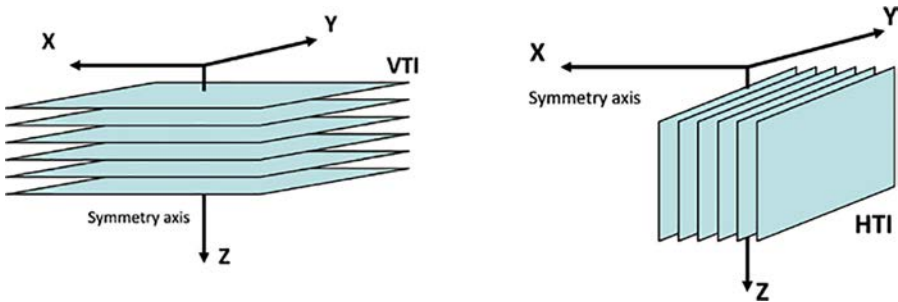


Figure 8.1 VTI (left) and HTI (right) to simplify the anisotropy modeling.

For *VTI media*, Thomsen introduced three variables (Thomsen, 2002), called *Thomsen parameters*,  $\epsilon$ ,  $\gamma$ , and  $\delta$ . In practice,  $\delta$  and  $\epsilon$  can be derived by adjusting the hyperbola during the NMO, using an additional term in the equation. As such, the VVAZ approach as presented in this chapter is also sensitive to this VTI configuration.

For *HTI media*, rock physics models, such as Mori-Tanaka (Mori and Tanaka, 1973), allow computing the elastic stiffness of an inclusion model, mixing some fracture apertures/orientations. Synthetic seismic data generated in 1D by such models allows us to draw general observations:

- Anisotropy is not detected at short offsets.
- If one fracture set is present, with a given orientation, a large fracture density and large fracture lengths, it leads to a measurable anisotropy in the seismic at large offset (or angle, around 30°).
- Two equivalent perpendicular fracture sets lead to isotropic result and kill the anisotropy effect; while changing the balance between both sets, the anisotropy intensifies at large offset or incidence angle.

In practice, not only faults and fractures can be detected using HTI media approximation. Any brutal and oriented change affecting the wave, such as a lithology or porosity change, can generate similar anisotropy. In addition, the *lateral resolution* is also a key factor: If an element is wide enough to be detected, regardless of the azimuth, no anisotropy will be induced.

### 8.1.2 Azimuthal stacking and required processing

In the previous chapter, the partial stacking was introduced to generate full-stack or angle-stacks from *gather*s. Another stacking method, to detect anisotropy, is possible with *Wide Azimuth (WAZ)* seismic acquisition and associated gathers using the *azimuthal key*, representing the direction between the line source/receptor and the north. As for the previous application, the gathers must be “*amplitude preserved*”.

The response of the signal is expected to be symmetrical: exchanging the location between the source and the receptor should lead to a similar signal. An azimuthal range of 0-30° is then equivalent to a range of 180–210°. This technique allows more traces to be involved during stacking, and, therefore, to reduce the *noise content* of the azimuthal stacks.

For the VVAZ approach, different alignment processes might destroy the expected anomalies, especially:

- All the azimuth dependent velocity picking or RNMO.
- The trim-statics, which is a process that aligns seismic events using dynamic shifts.
- Filters, such as Radon or F-K filters, might not be adapted to preserve the azimuthal information.

As the anisotropy is mostly detectable for the large offsets/angles (Chérel et al., 2010), these must be considered during the stack (even up to very large offsets, further than Aki-Richards classical limitations for elastic inversion workflows). This way, the chance to detect anisotropy would significantly increase.

## 8.2 Velocity versus Azimuth (VVAz): a shift detection methodology

The misalignments between the azimuthal stacks and the full-stack full-azimuth are very informative, as it can be translated as *velocity anomalies* (VVAZ). It is also key to correct them, enhancing the stack's compatibility before comparing their amplitude variations with the azimuth (AVAZ), to get an accurate estimation of such subtle effects.

The shift detection is performed on each *azimuthal stack* (anisotropic) taking a full-stack full-azimuth as reference (isotropic), as described in the previous chapter during the seismic data conditioning for seismic inversion.

The resulting dynamic shifts observed in each sector can be understood as velocity anomalies according to this “isotropic” velocity, associated to the full-stack. Different elements must be considered when choosing this parameter:

- The window for the shift detection must be put at its lowest as it controls the *vertical resolution* of the VVAZ anomaly.
- The induced interval variations must be computed, to QC their values. The parameter set must be refined using trials and errors to remain in realistic ranges.
- In areas where the signal is of low quality, the shift values must tend to zero, which implies no VVAZ effect.

The following sequence is proposed to obtain the interval velocities by azimuthal sector:

1. Compute the average velocity from the interval velocities (isotropic). It corresponds to the average of the interval velocities, in TWT domain.
2. Compute correction coefficients by sector:

$$\text{Coef} = \frac{\text{TWT} - \text{shift}}{V_{\text{avg}}}$$

3. As the depth of events is the same, the multiplication of such coefficients with the average velocities (isotropic) leads to corrected average velocities by azimuthal sector.
4. A Dix formula variation allows to estimate the interval velocities by azimuthal sector from the average velocities.

At the end of the process, as many interval velocity models as azimuthal stacks are obtained, from which anisotropy can be extracted.

### 8.3 Amplitude versus Azimuth (AVAz): an inversion methodology

Amplitudes are related to impedance contrasts rather than impedance itself. Consequently, it is preferred, for Amplitude variation versus Azimuth (AVAZ) methodology, to perform a series of *seismic inversions* (Al-Kandari et al., 2009), to evaluate the anisotropy of a key elastic property of the media, the P-impedance, on each azimuthal stack.

The method is the one described in the previous chapter, applied to *azimuthal stacks*. These stacks must contain information from large offsets to be able to detect anisotropy. In addition, as the amplitude is compared from one azimuthal stack to another, the events should be properly aligned before applying the processes.

To avoid introducing any bias related to the different azimuthal sectors, the key parameters should be defined using the full-stack full-azimuth seismic data:

- Unique optimal wavelet: initial shape, phase rotation, energy.
- Uniform well-to-seismic calibration: the wells are tied the same way to the seismic data. The synthetic at well does not model anisotropy.
- Unique prior model.
- Homogeneous inversion parameter set: the parameters are the same to ensure the same level of convergence of the algorithm.

At the end of the process, as many inverted P-impedance models as azimuthal stacks are obtained, from which the only difference comes from the signal itself.

### 8.4 Ellipse fitting on properties to estimate the anisotropy

Either for the velocity (VVAZ) or the impedance (AVAZ), the ellipse fitting allows to capture the variability of the property according to the azimuth (Adelinet et al., 2013). In polar coordinates, each sector response (for each cell, in 3D) is plotted as a point, for which the radius corresponds to the magnitude of the property, and the angle to the average azimuth angle, as displayed Figure 8.2.

An isotropic response, corresponding to the same magnitude for all angles, will result in a *circle*, while a different response will be approximated by an *ellipse*. This ellipse has two main parameters:

- The *orientation* of the major axis: corresponding to the orientation associated with the major magnitude of the property.
- The *ratio* of the axis: 1 for a circle, greater than 1 for anisotropy detection.

Compared to raw statistics such as variance, the ellipse fitting imposes anisotropy to be organized and oriented. It acts as a powerful denoising, and the orientation of the major axis is a key QC, supposed to be aligned with the fault/fracture orientations. For each source of information, the computation is performed in 3D, then extracted at key levels to evaluate the results, as illustrated in Figure 8.3.

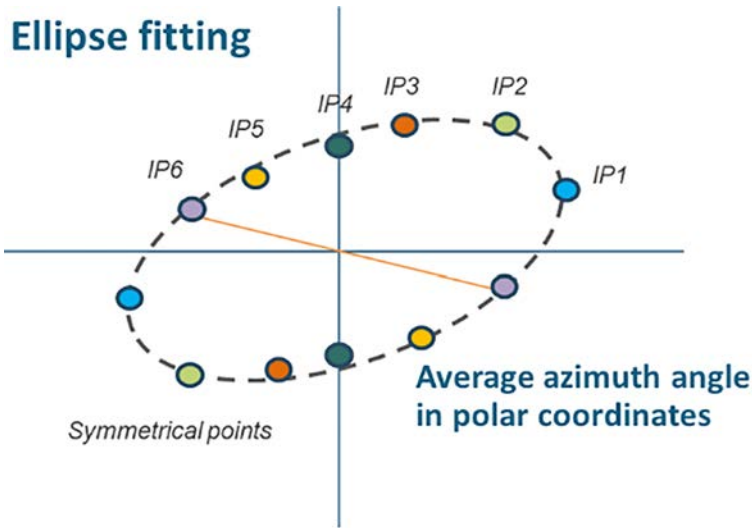


Figure 8.2 *Ellipse fitting to extract the anisotropy intensity and orientation.*

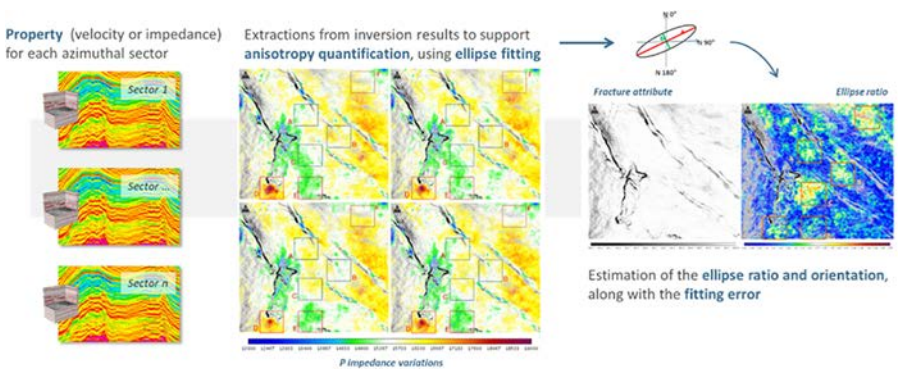


Figure 8.3 *Ellipse fitting, a powerful tool to combine maps into anisotropy estimation.*

## 8.5 From anisotropy to fracture attributes

The relationship between anisotropy and fracture is not direct; a lateral change of any property affecting the impedance (lithology, porosity, fluid, ...) may lead to the same effect. To derisk the anisotropy interpretation, a lateral gradient computed on each of these predicted properties should be calculated (Baillet et al., 2024). This attribute captures their lateral variation rate. Cut-off values can be proposed to mask the anisotropy anomalies where a property is changing too much; in remaining areas, the high anisotropy has been interpreted as fracture density. In the illustration below, Figure 8.4, the remaining high anisotropy, in red in the bottom section, are interpreted as fracture density from the original anisotropy volume, in colors in the top section.

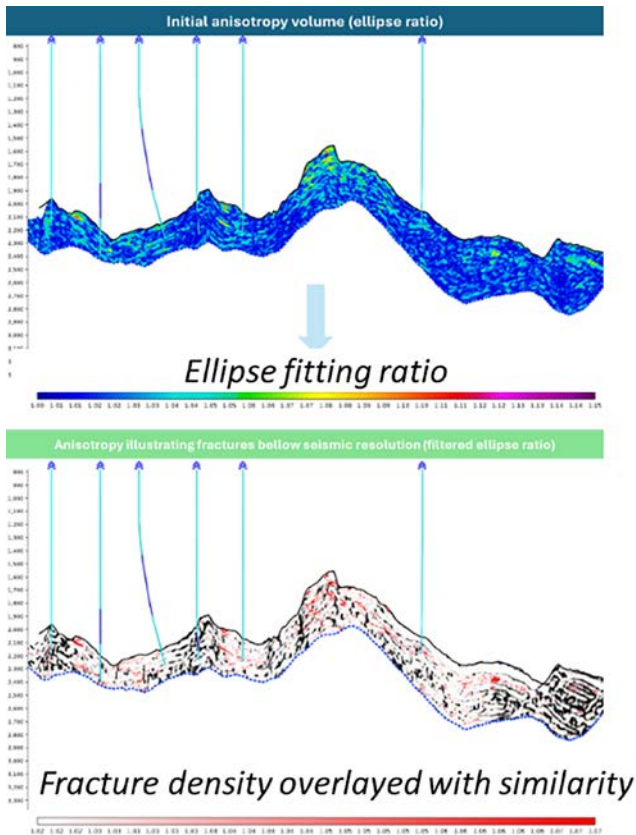


Figure 8.4 Example of derisking anisotropy attribute when other reservoir properties are stable.

## 8.6 Case study: Fracture characterization through azimuthal inversions to prospect the geothermal potential of Geneva basin

To develop the exploitation of geothermal resources in the city of Geneva, a prospection phase has been initiated to better characterize the basin with a newly acquired and processed 3D wide-azimuth land seismic. The Geneva basin location between alpine massifs south side and the Jura north side makes its geology complex and subject to variable constraints which enhanced geothermal energy development. The present project consists of an azimuthal anisotropy intensity analysis at different reservoir levels, to be related to more subtle fracture characterization than using conventional seismic attributes. In this project, both AVAZ and VVAZ approaches as described in this chapter are tested and compared.

### 8.6.1 Processing, conditioning, shift detection

CMP gathers are available at different processing stages, allowing the best choice that suits the needs of the study. The gathers with migration and isotropic NMO (Normal Move Out) have been selected; versions with steps such as trim statics and the Radon filter have been discarded as they might alter both the AVAZ and VVAZ responses.

To eliminate the surface waves, an outer time-variable mute is applied to the original gathers before stacking. As the anisotropy is mostly contained in the far offset traces, all the available data, regardless of the offset, has been considered. The stack generation tests showed the possibility to get 6 azimuthal stacks (Table 8.1), enhancing therefore the possibility to detect anisotropy and the accuracy of its orientation.

Table 8.1 Ranges of the azimuthal stacks.

Name	Full-stack	AZ1	AZ2	AZ3	AZ4	AZ5	AZ6
Range	0–180°	15–45°	45–75°	75–105°	105–135°	135–165°	165–205°

The noise-to-signal ratio is enhanced by considering symmetrical azimuthal ranges; the seismic response varies with the direction source-receptor, regardless of the orientation. Remaining noise content can be managed through the model-based inversions (AVAZ) or the probe size during shift detection (VVAZ).

In addition, full-stack full-azimuth seismic data has been generated as a reference. The following maps (Figure 8.5) illustrate, as QCs, the correlation map (left) and the RMS map (right), highlighting the area of the survey, covering Geneva city. Part of the survey is offshore (in the Lemman Lake), and part of the seismic data is noisier below the city, as visible in both maps.

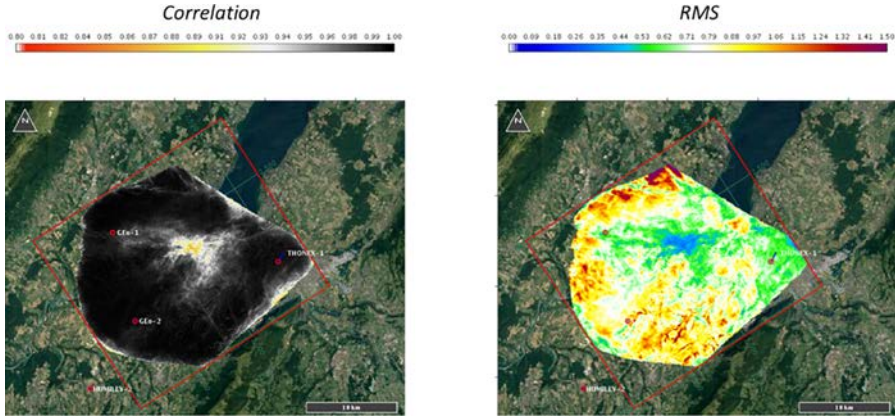


Figure 8.5 Correlation (left) and energy (right) map computed on the full stack

As a base for the VVAZ approach, isotropic interval velocities from RMS velocities have been deduced through Dix formula (Figure 8.6). Trials and errors have been used to set the interval parameter to 40 ms; beyond, the obtained velocities are less accurate, below, the obtained velocities contain gridding artifacts, as observable, attesting of the too high sampling compared to the original RMS picking.

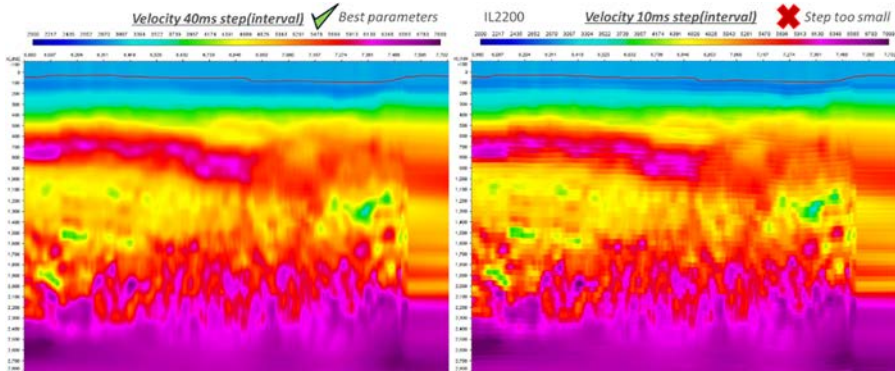


Figure 8.6 interval velocity using Dix formula for 40 ms (left) and for 10 ms (right).

While aligning the stacks, detecting shifts according to the reference, tests (errors and trials) have been undertaken to establish the final parameters. As displayed in Figure 8.7, the shifts obtained are subtle, mainly between  $\pm 5$  ms. They are directly linked to the average velocities, while their vertical gradients are linked to the interval velocities. Therefore, constant shifts (vertically) indicate no anomaly, while abrupt (vertical) changes indicate a presence of VVAZ anomaly.

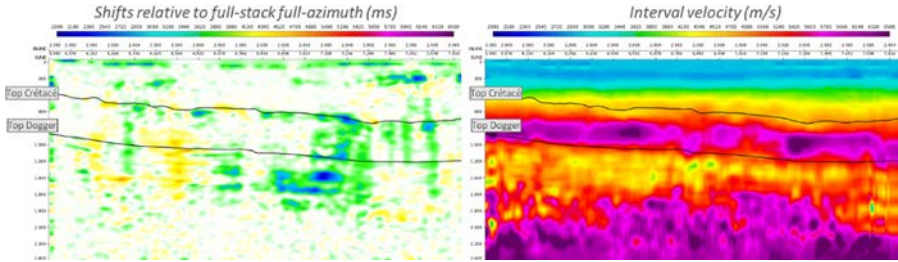


Figure 8.7 Shifts detected in milliseconds (left) converted to interval velocity (right) for an azimuthal sector.

Some observations can be made:

- The shifts detected are different from one azimuthal sector to another, already revealing VVAZ effects.
- The shift main shift changes (except the shallow weather zone) are located at the Top Cretaceous level.

In the end, the procedure to derive interval velocities from the shift volume has been applied to the 6 azimuthal stacks, ready to extract the VVAZ anisotropy.

### 8.6.2 Model-based inversions

The azimuthal stacks have been aligned using the detected optimal shifts to optimize their mutual compatibility, for estimating properly the AVAZ effects. Then, to obtain P-impedance model by sector, a series of model-based seismic inversions is performed. To illustrate, an optimized impedance section, for one sector, is proposed Figure 8.8.

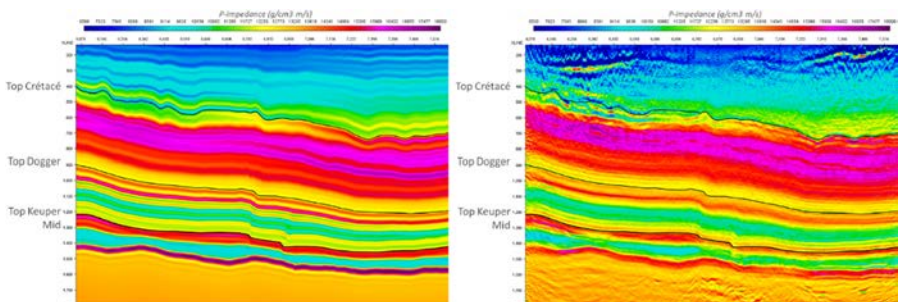


Figure 8.8 P-impedance section from the prior model (left) and after inversion for stack 1 (right).

Although acoustic inversion technique has been selected, the obtained property can be considered as a “pseudo-P-impedance”, as large offset traces will have more contribution than short offset traces in the amplitude variations, to better capture the anisotropy.

The convergence for the azimuthal stacks varies from 70% to 80%, in accordance with the initial level of noise of each azimuthal stack. The noise, discarded from the synthetic seismic and observable in the residuals, hasn't been included in the 6 optimized impedance models, in order to better estimate the AVAZ effects.

### 8.6.3 Results and way forward

Either for the VVAZ or the AVAZ approach, the focus is based on the variation of the properties with the azimuth rather than their absolute values. In both approaches, the anisotropy has been extracted using ellipse fitting: an isotropic response would result in a circle, while a different response would be approximated by an ellipse, with two main parameters: (1) the orientation of the major axis, corresponding to the tilt associated with the major magnitude of the property (usually parallel to the fractures), (2) the ratio of the axis, greater than 1 for anisotropy detection.

While comparing the results obtained in sections, Figure 8.9, it is observable that:

- The anisotropy from VVAZ is more subtle than AVAZ, so that the scale has been saturated for display purposes.
- The resolution of the anisotropy from AVAZ (right) seems to be better than the VVAZ (left).
- Some anisotropic areas, especially around the Top Cretaceous or the Top Keuper, seem to correlate between both methods, while others don't.
- Where there is no signal, especially around the major fault at the center part of the section, no anisotropy is detected (VVAZ or AVAZ).

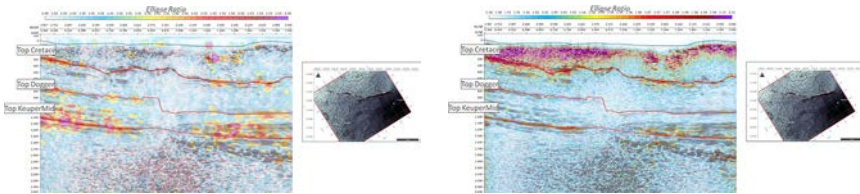


Figure 8.9 Anisotropy in section, VVAZ (left) and AVAZ (right).

At low depth, as illustrated Figure 8.10 in time slice (700 ms), both approaches are compatible with each other, focusing on objects with apparently the same size and resolution.

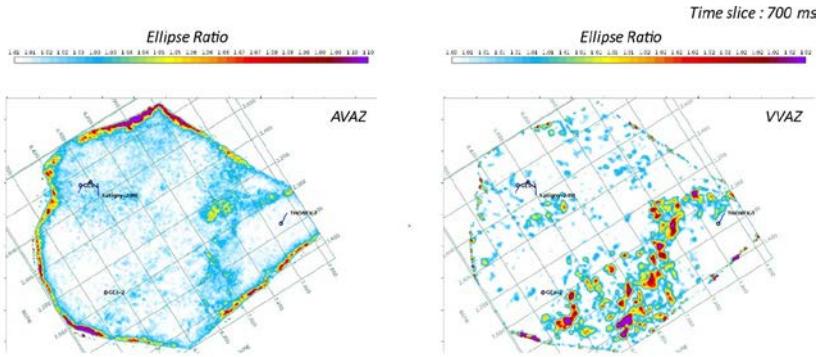


Figure 8.10 AVAZ (left) and VVAZ (right) anisotropy at 700 ms time slice.

The same visual can be performed highlighting the areas with no signal (low energy) and conventional fracture attributes (3D similarity), Figure 8.11. The low energy areas, in pink, indicate no information rather than no anisotropy. The conventional fracture attributes, in black, indicate the presence of faults and fractures at greater scale, completing the understanding of the anisotropy distribution. In these maps, some blocks between major faults can be affected or not by anisotropy, which may indicate the presence or absence of fractures.

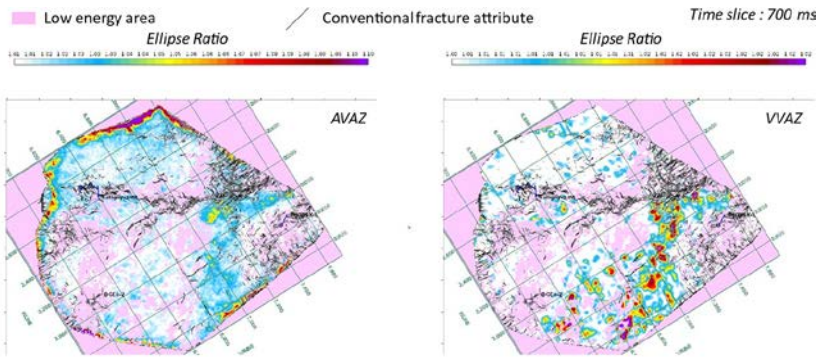


Figure 8.11 AVAZ (left) and VVAZ (right) anisotropy at 700 ms time slice, with weak signal areas in pink.

From Top Cretaceous to Top Dogger, The AVAZ results highlight similar areas (Figure 8.12), while VVAZ results vary at these same levels (Figure 8.13), indicating a poor compatibility between AVAZ and VVAZ.

The strong amplitudes of the Top Cretaceous may affect the deeper events, showing therefore similar anomaly areas. The VVAZ does not depend on this amplitude effect and may be more reliable from below the Top Cretaceous down to the Top Dogger.

The compatibility between the attributes is again observable from the Top Keuper Mid horizon and below (Figure 8.14).

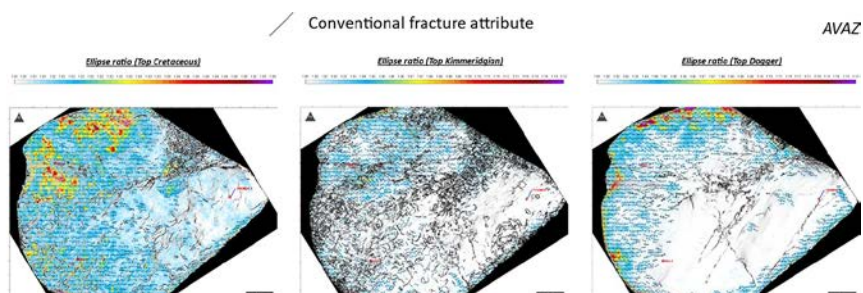


Figure 8.12 AVAZ anisotropy at Top Cretaceous (left), Top Kimmeridgian (middle) and Top Dogger (right).

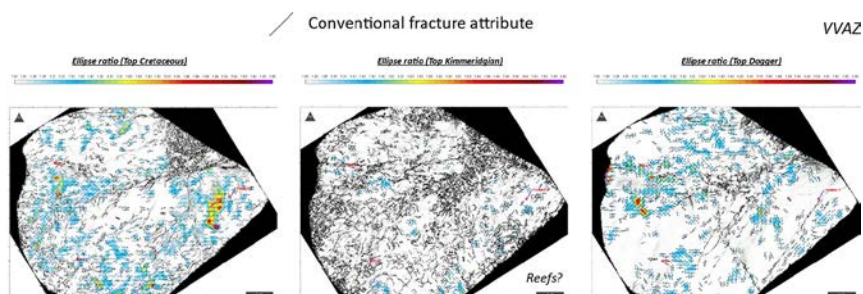


Figure 8.13 VVAZ anisotropy at Top Cretaceous (left), Top Kimmeridgian (middle) and Top Dogger (right).

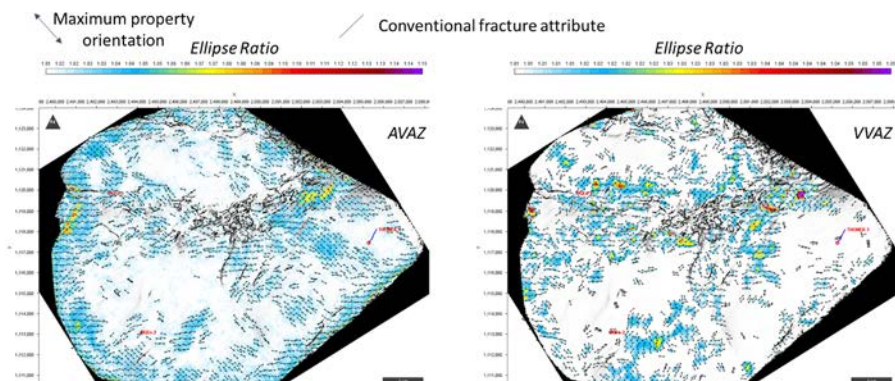


Figure 8.14 AVAZ (left) and VVAZ (right) anisotropy at Top Keuper Mid level.

## Conclusions and perspectives

The work described in this chapter has been applied using newly generated azimuthal stacks, for which the processing sequence has been evaluated very carefully, preventing destructive steps for both AVAZ and VVAZ approaches. When both approaches seem equally acceptable, as along the Top Cretaceous event, labelling depending on the anisotropy range is proposed for AVAZ and VVAZ approaches (Figure 8.15) using cut-offs, and the result would highlight, in red, the most prospective areas outside low-energy areas and outside main seismic faults.

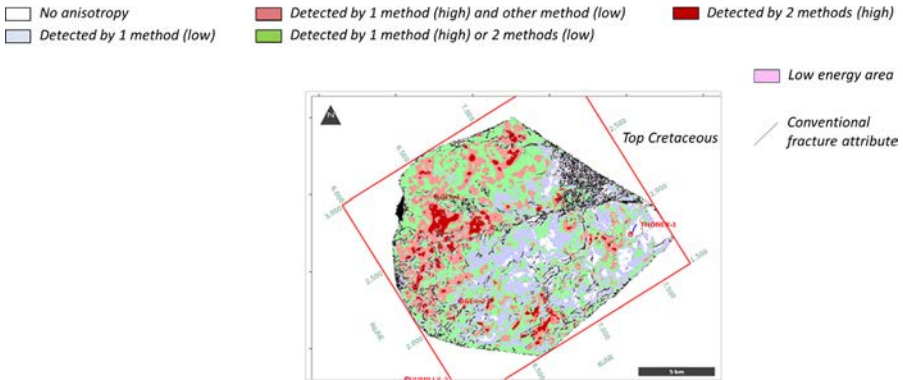


Figure 8.15 *Ellipse fitting, a powerful tool to combine maps into anisotropy estimation.*

The anisotropy interpretation as a fracture attribute is still a challenge. A brutal and oriented change in properties affecting impedance, such as karsts, can also induce anisotropy. As a way forward, matrix characterization and karst identification will be carried out to further understand the other possible anisotropy sources, using elastic inversion as described in the previous chapter. Still in exploration phase, the new wells to be drilled in the area will reveal key aspects to refine the anisotropy interpretation, using BHI to interpret the fault and fracture clusters to be correlated with the anisotropy results.

## References

Adelinet M., Barnoud A., Clochard V., Ricarte P. (2013) Improved unconventional reservoir characterization using multi-azimuth stratigraphic inversion, case

- study on the Fort Worth Basin, *Journal of Unconventional Oil and Gas Resources* 3-4, 15-26, <https://doi.org/10.1016/j.juogr.2013.10.001>.
- Adelinet M., Clochard V., Barthelemy J.F., Chérel L. (2012) Determination of Crack Orientation in a Fractured Reservoir from Effective Medium Modelling and Multi-azimuth Inversion, 74th EAGE Conference and Exhibition incorporating EUROPEC 2012, cp-293-00564.
- Al-Kandari A., Kumar R., Convert P., Ortet S., Lecante G. (2009) Fracture characterization using seismic data in a West Kuwait field, *SEG Technical Program Expanded Abstracts* 2009, 1775-1779, <https://doi.org/10.1190/1.3255197>.
- Baillet R., Caudroit J. (2024) Seismic fracture characterization using AVAZ and VVAZ anisotropy for geothermal prospection in the Geneva basin, Switzerland, 85th EAGE Annual Conference & Exhibition, Oslo, Norway.
- Baillet R., de Freslon N., Thomas V., Castellanos R., Denogean E. (2024) Fracture and matrix characterization using wide-azimuth and multi-component seismic data: A case study from offshore Mexico, *SEG Technical Program Expanded Abstracts* 2024, 144-148, <https://doi.org/10.1190/image2024-4101418.1>.
- Chérel L., Bruneau J., Dubos-Sallée N., Labat K., Barthelemy J.F., Daniel J.M. (2010) Understanding seismic anisotropy from fractures observed in wells, 72nd EAGE Conference.
- Elapavuluri P., C.J. Bancroft (2002) Estimation of Thomsen's Anisotropy Parameter  $\delta$  and  $\epsilon$  Using EO Gather, *Crewes Research Report* 14, 18.
- Liu E., Martinez A. (2012) Seismic Fracture Characterization: Concepts and Practical Applications, EAGE Publications.
- Mori T., Tanaka K. (1973) Average stress in matrix and average elastic energy of materials with misfitting inclusions, *Acta Metall.* 21, 571-574.
- Thomsen L. (2002) Understanding seismic anisotropy in exploration and exploitation: SEG-EAGE Distinguished Instructor Series No. 5, SEG.